

Nonlocal Optical-Model Analysis of Neutron Scattering from Nuclei Near $A = 100$ at Energies Below 1 MeV*

A. J. ELWYN, R. O. LANE, A. LANGSDORF, JR., AND J. E. MONAHAN

Argonne National Laboratory, Argonne, Illinois

(Received 15 August 1963)

The polarization and differential cross sections for neutrons scattered from the nuclei Zr, Nb, Mo, and Cd have been measured at five angles for neutron energies between 0.275 and 0.85 MeV. The results have been analyzed in terms of an optical model equivalent to the nonlocal model of Perey and Buck. The analysis leads to the following conclusions: (1) The calculations, corrected for the effects of compound elastic scattering, are consistent with most of the scattering data when a spin-orbit potential that includes both a real ($V_s \approx 10$ MeV) and an imaginary ($W_s \approx 4$ MeV) term of the Thomas type is employed. (2) As calculated on the basis of this model, the magnitude and shape of the P -wave neutron strength-function peak in the region near $A = 100$ are rather insensitive to the values chosen for the real and imaginary spin-orbit potentials—at least for $7.2 \leq V_s \leq 20$ MeV and $0 \leq W_s \leq 7.2$ MeV. Thus, on the basis of this model the possible splitting of the $3P$ strength function peak cannot be interpreted in terms of a spin-orbit force.

I. INTRODUCTION

THE optical model has been quite successful in accounting for the average behavior observed in the elastic scattering of neutrons from nuclei, particularly in the energy range above 5 MeV. At low energies, however, specifically at energies below 1 MeV, the paucity of systematic experimental data on neutron polarization, and the strong dependence of the calculations on the methods of treating compound-nucleus effects have made it difficult to obtain a completely consistent interpretation of the average neutron-nucleus interaction.

A reasonably complete evaluation of an optical model requires that the energy dependence and angular dependence of the differential cross section and polarization be systematically measured as a function of mass number and compared with the predictions of the model. The polarization, in particular, is quite sensitive to the strength of the spin-orbit coupling in the interaction. Its systematic study, therefore, might lead to a determination not only of the magnitude but also of the radial dependence of the spin-orbit potential. Further, any acceptable optical-model description of neutron scattering must be consistent with measured total cross sections and with measured values of the S - and P -wave neutron strength functions.

Most optical-model calculations predict a P -wave giant resonance in the neutron total cross section (and in the P -wave neutron strength function) at mass numbers around $A = 100$. The polarization of neutrons scattered from nuclei in this mass region has previously been measured by Adair *et al.*¹ and Clement *et al.*² at energies of 0.38 and 0.98 MeV at a few scattering angles. These results confirmed that, at least at a few angles, the polarization reaches a maximum near $A = 100$. Early attempts to interpret these measurements in terms of a

square-well optical potential plus a real spin-orbit term were not very satisfactory.² Nemirovskii,³ who analyzed these data with a diffuse potential well with volume absorption and a real surface spin-orbit term, obtained reasonable agreement with the 0.38-MeV results. Further analysis of the 0.98-MeV data by Bjorklund,⁴ who used a diffuse potential well with surface absorption and a real spin-orbit term of the Thomas form, did not lead to a systematic interpretation of the results. It should be mentioned that the sign of the spin-orbit term in the original Bjorklund-Fernbach potential⁵ has been shown to be opposite to that required by the shell model.⁶

Recently Brown *et al.*⁷ have measured the polarization of neutrons scattered from Cd at 55° and from Mo at 55° and 90° at energies from 0.3 to 1.5 MeV. Hooten⁸ used the Bjorklund-Fernbach diffuse-potential model to analyze these results. His calculations, corrected for the effects of compound elastic scattering, were in only approximate agreement with the data.

The most systematic experimental data on the unpolarized differential cross sections of neutrons scattered from a large number of nuclei at energies below 1 MeV are the results of Lane *et al.*^{9,10} Further measurements in this energy range and at mass numbers near $A = 100$ have been made by Reitmann *et al.*¹¹ The recent

³ P. E. Nemirovskii, Zh. Eksperim. i Teor. Fiz. **36**, 588 (1959) [translation: Soviet Phys.—JETP **9**, 408 (1959)].

⁴ F. Bjorklund, *Proceedings of the International Conference on the Nuclear Optical Model, Florida State University Studies, No. 32* (The Florida State University, Tallahassee, Florida, 1959), p. 1.

⁵ F. Bjorklund and S. Fernbach, Phys. Rev. **109**, 1295 (1958).

⁶ C. Wong, J. D. Anderson, J. M. McClure, and B. D. Walker, Phys. Rev. **128**, 2339 (1962); P. Moldauer (private communication).

⁷ D. Brown, A. T. G. Ferguson, and R. E. White, Nucl. Phys. **25**, 604 (1961).

⁸ D. J. Hooten, Phys. Rev. **128**, 1805 (1962).

⁹ A. Langsdorf, Jr., R. O. Lane, and J. E. Monahan, Phys. Rev. **107**, 1077 (1957).

¹⁰ R. O. Lane, A. Langsdorf, Jr., J. E. Monahan, and A. J. Elwyn, Ann. Phys. (N. Y.) **12**, 135 (1961).

¹¹ D. Reitmann, C. A. Engelbrecht, and A. B. Smith, Nucl. Phys. (to be published).

* Work performed under the auspices of the United States Atomic Energy Commission.

¹ R. K. Adair, S. E. Darden, and R. E. Fields, Phys. Rev. **96**, 503 (1954).

² J. D. Clement, F. Boreli, S. E. Darden, W. Haerberli, and H. R. Striebel, Nucl. Phys. **6**, 177 (1958).

compilation BNL-400¹² gives an extensive list of references to all previous results on differential cross sections. Moldauer¹³ has recently analyzed neutron-scattering and absorption data by use of a local diffuse-surface optical model having a sharply peaked absorptive shell on the nuclear surface. He was able to obtain consistent fits to low-energy differential and total cross sections, and to the *S*-wave neutron strength functions in the mass number interval $40 \leq A \leq 130$.

The present paper describes the results of an experiment to study the polarization and the unpolarized differential cross section for neutrons scattered from four nuclides, namely, Zr, Nb, Mo, and Cd, in the mass region of the giant $3P$ resonance. These measurements made at five angles for neutron energies between 0.275 and 0.85 MeV, were carried out in the belief that a systematic investigation would lead to a more consistent interpretation in terms of an optical model for neutron energies below 1 MeV.

The results in the present report are compared with calculations based on the recently proposed nonlocal optical model of Perey and Buck.¹⁴ This model has been shown to be quite successful in accounting for a variety of experimental data on neutron scattering at energies between 4 and 25 MeV, and to be at least in qualitative agreement with results at lower energies when the effects of compound elastic scattering are taken into account. In this model, which represents possibly a more realistic treatment of the interactions of nucleons in nuclear matter, the energy dependence of previous local-model fits to scattering data can be accounted for in large part by the use of energy-independent parameters that characterize the form factor of the nonlocal potential.

Although our efforts were directed mainly toward comparing the model directly with the data, preliminary modifications of some of the parameters were investigated. The polarization measurements in particular were analyzed in terms of a spin-orbit force having both a real and an imaginary term. A nonzero value for the imaginary term would indicate that neutron absorption depends at least partly on the same forces that bring about nuclear polarization.¹⁵ The introduction of a complex spin-orbit potential to describe neutron scattering at energies near 1 MeV has not previously been believed necessary.⁴

As mentioned above, an optical-model interpretation of scattering data must be consistent with absorption data. Hence, the predictions of the nonlocal model are compared with neutron strength functions, particularly the measured *P*-wave strength functions in the region of $A = 100$. Some attempts to explain a possible splitting of

the *P*-wave resonance in terms of a spin-orbit force are discussed in Sec. IV.B. 4.

II. EXPERIMENT

The experimental arrangement has been described previously (see Elwyn *et al.*¹⁶ and the other references listed therein), and therefore will be discussed only briefly here.

The source of polarized neutrons was the $\text{Li}^7(p,n)\text{Be}^7$ reaction, the incident protons being accelerated by the Argonne 4.5-MeV Van de Graaff generator. The neutrons, emitted at 51° relative to the direction of the incident proton beam, were produced from lithium metal or lithium nitride targets whose thicknesses (as measured by the rise-curve method at threshold) varied between 40 and 80 keV for 1.9-MeV protons. After passing between the poles of an electromagnet, the partially polarized neutrons impinged on slab-shaped scatterers not more than $\frac{1}{8}$ in. thick. The scattering samples were Zr, Nb, Mo, and Cd containing the normal isotopic abundances. The scattered neutrons were detected by banks of shielded BF_3 counters in an oil moderator; a shielded tank containing two BF_3 oil-moderated counters served as a monitor to sample the forward neutron flux. For this experiment five separate detectors were set at laboratory angles of 24° , 56° , 86° , 118° , and 150° on a circular track surrounding the position of the scattering samples. The neutron energies at which the polarization and differential cross sections were measured were 0.275, 0.35, 0.4, 0.45, 0.51, 0.55, 0.6, 0.65, 0.7, 0.75, 0.8, and 0.85 MeV.

For each scatterer at each neutron energy, the procedure was as follows. The intensity of scattered neutrons (the counting rate) was measured simultaneously at the five angles, first with the electromagnet turned off, and then with the magnet turned on at a value of magnetic field sufficient to precess the neutron spin through 180° . At each energy, the background with no scatterer in place was measured with the precessing magnet off, then with it on. At each scattering angle θ , the ratio $r(\theta)$ of the magnet-off to the magnet-on values of the net counting rates (the gross counting rate minus the properly normalized background counting rate) is equivalent to the usual left-right asymmetry ratio $L(\theta)/R(\theta)$. Here $L(\theta)$ and $R(\theta)$ would be the net counting rates for two detectors set at the same scattering angles to the right and left of the incident beam. This ratio is related to the product of the polarizations, $P_1(51^\circ)P_2(\theta)$, by the equation

$$P_1(51^\circ)P_2(\theta) = \frac{R(\theta) - L(\theta)}{R(\theta) + L(\theta)} = \frac{1 - r(\theta)}{1 + r(\theta)}, \quad (1)$$

where $P_1(51^\circ)$ is the polarization in the $\text{Li}^7(p,n)\text{Be}^7$ reaction at 51° , and $P_2(\theta)$ is the polarization that would

¹² M. D. Goldberg, V. M. May, and J. R. Stehn, *Angular Distributions in Neutron-Induced Reactions* (Office of Technical Services, Dept. of Commerce, Washington, D. C., 1962), 2nd ed., Vols. I and II, BNL-400.

¹³ P. Moldauer, *Nucl. Phys.* **47**, 65 (1963).

¹⁴ F. Perey and B. Buck, *Nucl. Phys.* **32**, 353 (1962).

¹⁵ W. Heckrotte, *Phys. Rev.* **101**, 1406 (1956).

¹⁶ A. J. Elwyn, R. O. Lane, and A. Langsdorf, Jr., *Phys. Rev.* **128**, 779 (1962).

arise if unpolarized neutrons incident on the scatterer were scattered at an angle θ . Further, the sum of the net counts with the magnet off and then on, which is equivalent to $L(\theta)+R(\theta)$, is directly proportional to the unpolarized differential cross section. The algebraic signs of polarizations $P_1(51^\circ)$ and $P_2(\theta)$ are chosen in accordance with the Basel convention,¹⁷ i.e., the polarization is positive in the direction defined by $\mathbf{k}_{in} \times \mathbf{k}_{out}$, where \mathbf{k}_{in} and \mathbf{k}_{out} are the wave vectors of the incident and outgoing particles, respectively, at the point of each interaction.

In the present experiment, the background counting rates were low. For each of the scatterers, the counting rate with no scatterer in place was not more than 10% of the rate with the scatterer in place at all angles less than 90° . At angles greater than 90° , for some of the samples the backgrounds approached 18% of the gross counting rate with scatterer in place.

III. DATA ANALYSIS AND RESULTS

Since the detectors could not distinguish elastically scattered neutrons from those of lower energy, both the $P_1(51^\circ)P_2(\theta)$ products and the unpolarized yields $L(\theta)+R(\theta)$ were corrected for the effects of the neutrons from the $\text{Li}^7(p,n)\text{Be}^7$ reaction leading to a state in Be^7 at 0.43 MeV,¹⁸ the assumption being that these neutrons were unpolarized.¹⁹ Inelastic scattering was considered to be negligible at the energies utilized in the present experiment. No attempt was made to correct any of these data for inelastic scattering. The unpolarized yields were also corrected for the relative nonuniformity of the five detectors and for the energy dependence of the response of any given detector.^{10,16} Absolute differential cross sections were obtained from the corrected normalized yields by use of smooth curves drawn through the previously measured neutron total cross sections obtained from the compilation in BNL-325.²⁰

The differential cross sections were corrected for the effects of multiple scattering by use of a Monte Carlo technique.²¹ The $P_1(51^\circ)P_2(\theta)$ products were corrected approximately for such effects under the assumption that second and higher order scatterings are unpolarized. The method has been described previously.²² In the present experiment this procedure probably tends to overcorrect the data; the true values of the polarization lie between the corrected and uncorrected values. In any event, the corrected values usually differ from the uncorrected ones by less than the statistical error.

¹⁷ *Proceeding of the International Symposium on Polarization Phenomena of Nucleons, Basel, 1960* [Suppl. Helv. Phys. Acta 6, 436 (1961)].

¹⁸ A. B. Smith (private communication); P. R. Bevington, W. W. Rolland, and H. W. Lewis, *Phys. Rev.* **121**, 861 (1961).

¹⁹ L. Cranberg, *Phys. Rev.* **114**, 174 (1959).

²⁰ D. J. Hughes and J. A. Harvey, *Neutron Cross Sections, BNL-325 and Supplement* (Superintendent of Documents, U.S. Government Printing Office, Washington, D.C., 1955 and 1957).

²¹ R. O. Lane and W. F. Miller, *Nucl. Instr. Methods* **16**, 1 (1962).

²² A. J. Elwyn and R. O. Lane, *Nucl. Phys.* **31**, 78 (1962).

Other systematic effects which might lead to spurious asymmetries in the magnet-off and magnet-on measurements are believed to be small. Effects due to the finite size of the scatterer and detector²³ cancel completely since a magnetic field is used to rotate the neutron spins. Also, possible depolarization effects connected with the use of a magnetic field have been found to be negligible.¹⁶ In a supplementary experiment performed at one energy (0.7 MeV), the left-right measurements with two detectors set up at equal scattering angles to the left and right of the 0° direction were compared with the "magnet on"–"magnet off" measurements. We were especially concerned with possible systematic effects at the smallest scattering angle (24°). For some cases, the measured values of $P_1(51^\circ)P_2(24^\circ)$ appeared to be quite large relative to those of $P_1(51^\circ)P_2(56^\circ)$. The results (obtained with high statistical accuracy) indicated that no large systematic effects were present and indeed confirmed the original small-angle measurements within their statistical uncertainties.

Finally, the values of $P_2(\theta)$ were obtained from the measured products $P_1(51^\circ)P_2(\theta)$ by use of previously

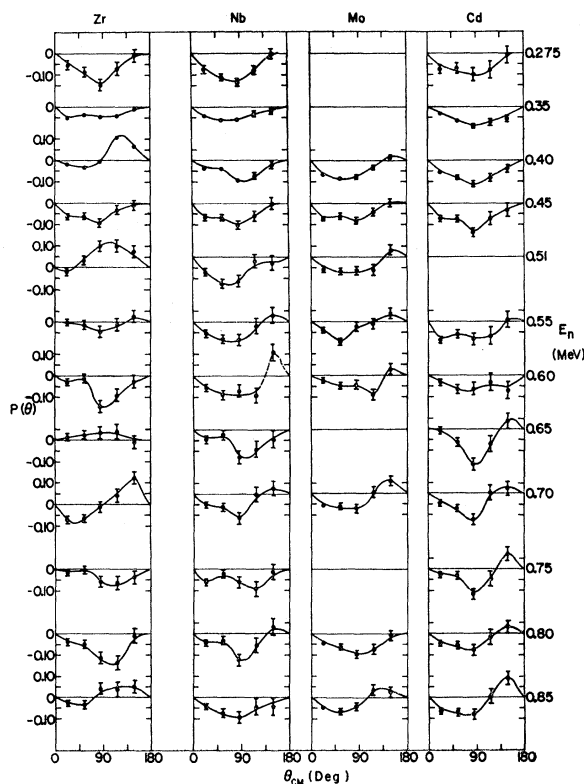


FIG. 1. The polarization $P(\theta)$ as a function of angle for each incident-neutron energy for the nuclides Zr, Nb, Mo, and Cd. The solid curves are drawn as a visual aid only. In this figure the points have not been corrected for multiple scattering.

²³ J. E. Monahan and A. J. Elwyn, *Nucl. Instr. Methods* **14**, 348 (1961); J. E. Evans, Atomic Energy Research Establishment Report AERE-R3347, 1960 (unpublished).

measured values for $P_1(51^\circ)$.²² These values of $P_1(51^\circ)$ were averaged over the energy spread of the beam (40–80 keV) by use of the known values of the differential cross sections²⁴ at 51° for the $\text{Li}^7(p,n)\text{Be}^7$ reaction. The final values of $P_2(\theta)$ are also to be interpreted as average values.

The complete results, both differential cross sections and polarizations, are available in tabular form from the authors. The errors on the final results are statistical only; for the values of $P_2(\theta)$ they do not include errors associated with the determination of $P_1(51^\circ)$.

IV. DISCUSSION

A. Present Results

The polarization $P_2(\theta)$ as a function of angle for each incident-neutron energy is shown in Fig. 1 for all four nuclei. The results for Nb, Mo, and Cd are similar both in sign and magnitude throughout the energy region studied with only a few exceptions. In particular we might note that the polarization for the niobium nucleus (mass number $A=93$) has the same sign at all angles (except at $\theta=150^\circ$) as that for the cadmium nucleus ($A=112$). In the energy range studied in the present experiment, therefore, it is quite likely that the polarization (at most angles) does not change sign from mass number $A=93$ to $A=112$.²⁵

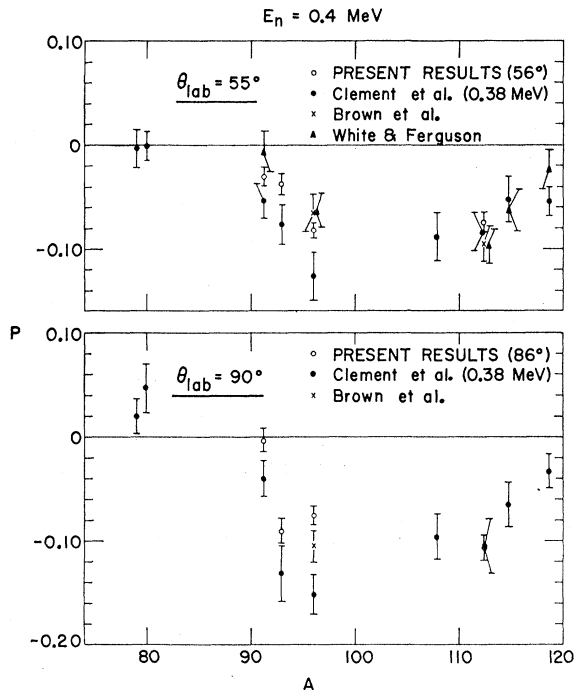


FIG. 2. The polarization P as a function of mass number A . The present measurements of P at an incident-neutron energy of 0.4 MeV for laboratory angles of 56° and 86° are compared with previous results (Clement *et al.*, Ref. 2; Brown *et al.*, Ref. 7; and White and Ferguson, Ref. 27).

²⁴ S. M. Austin, Bull. Am. Phys. Soc. 7, 269 (1962).

²⁵ This statement should of course be checked experimentally by studying the polarization of other nuclei in the mass-number range $96 < A < 112$.

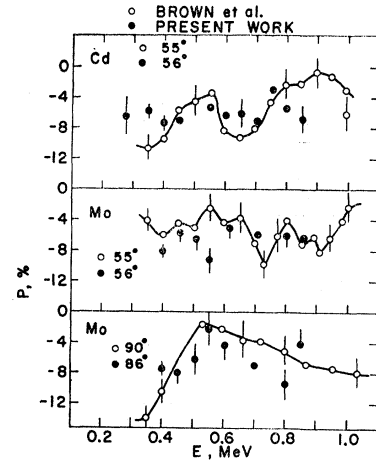


FIG. 3. Polarization as a function of energy for Cd at 56° and for Mo at 56° and 86° . The present measurements are compared with those of Brown *et al.* (Ref. 7). The solid curve through the results of Brown *et al.* has been drawn as a visual aid only.

For Zr (Fig. 1), however, the polarization fluctuates in sign as well as in magnitude as a function of incident energy. Previous experiments^{11,26} have shown that the total cross section is likewise not a smooth function of energy. Since the major isotope Zr^{90} has a magic number of neutrons ($N=50$), we might expect that the isotopes of Zr (especially Zr^{91}) have broad and well-spaced energy levels. Even with the resolution used in the present experiment, therefore, it is perhaps not surprising that the measured polarizations fluctuate rapidly with energy. If the values of $P_2(\theta)$ for Zr are averaged over larger energy intervals, the gross fluctuations are smoothed out considerably and the averaged results are more in agreement with the behavior of the other nuclei, although the values of $P_2(\theta)$ are slightly smaller in all cases (see Sec. IV.B.2).

The polarization produced by scattering from nuclei with mass numbers near $A=100$ at a few of the energies and angles involved in the present study has previously been measured at Wisconsin by Clement *et al.*² and at Harwell by Brown *et al.*⁷ and by White and Ferguson.²⁷ Figure 2 shows these results near 0.4 MeV for the two laboratory angles 55° and 90° . All of the measured results are in good agreement. Excellent agreement is also found between the present results and those of White and Ferguson²⁷ for Mo and Cd at 55° and 0.7 MeV.

Brown *et al.*⁷ have studied the energy dependence of the polarization in scattering from Mo and Cd at 55° and Mo at 90° . Figure 3 compares some of their results with the present measurements on these two nuclei. It has been suggested⁸ that the rapid fluctuations of the polarization with energy observed in the Harwell work, especially for Cd at 55° and Mo at 90° , show a significant systematic trend. Although the present results are in good general agreement with the Harwell measurements (both in sign and magnitude), within their statis-

²⁶ C. K. Bockelman, R. E. Peterson, R. K. Adair, and H. H. Barshall, Phys. Rev. 76, 277 (1949).

²⁷ R. E. White and A. T. G. Ferguson, Nucl. Phys. (to be published). We thank Professor H. H. Barshall for communicating these results to us.

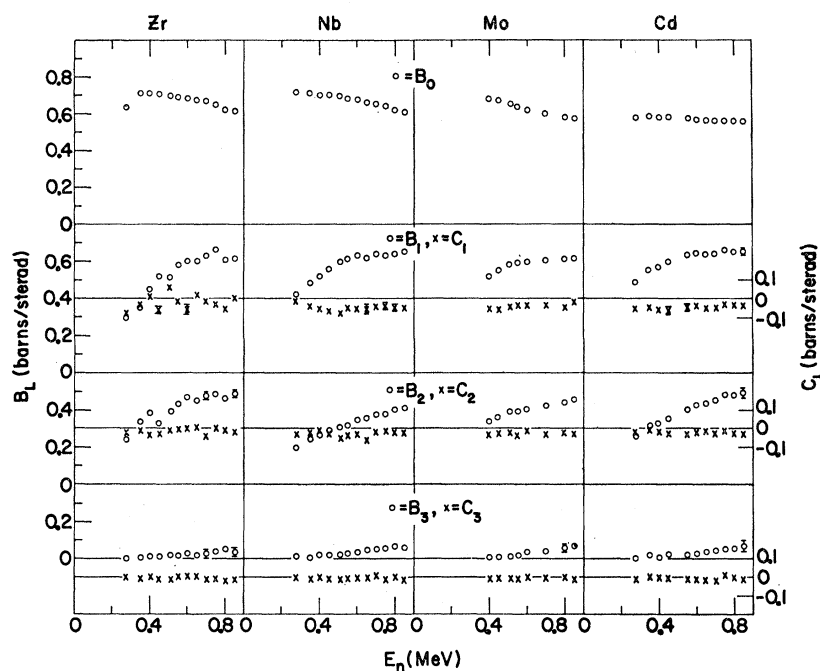


FIG. 4. Energy dependence of the coefficients B_L in the expansion of the unpolarized differential cross sections $\sigma(\theta)$ into a series of Legendre polynomials, and the coefficients C_L in the expansion of the product $\sigma(\theta)P_2(\theta)$ into a series of associated Legendre polynomials of the first order for the nuclides Zr, Nb, Mo, and Cd. The left-hand ordinate refers to the values of B_L (open circles); the right-hand ordinate to the values of C_L (\times 's). Note that the zeros for the right-hand and left-hand ordinates do not coincide.

tical accuracy our data do not indicate the rather rapid variation with energy that seems to characterize the Harwell work. A possible exception is found for Mo at 86° ; but even here the present results do not show the more dramatic energy dependence of the previous work.

The unpolarized differential cross sections obtained at the same time as the polarization are shown in Fig. 4. These data are given in terms of the coefficients B_L in a Legendre polynomial expansion

$$\sigma(\theta) = \sum_{L=0}^3 B_L \mathcal{P}_L(\cos\theta). \quad (2)$$

Also shown on the same graph (as open circles) are the coefficients C_L in the expansion

$$\sigma(\theta)P_2(\theta) = \sum_{L=1}^3 C_L \mathcal{P}_L^1(\cos\theta), \quad (3)$$

in which the product $P_2(\theta)\sigma(\theta)$ is expressed as a series of associated Legendre polynomials of the first order. Both sets of coefficients, B_L and C_L , were determined by a least-squares analysis of the data in terms of expansions (2) and (3).

The coefficient B_0 is equal to $\sigma_t/4\pi$. The values of B_0 shown in the figure are, therefore, proportional to the values of total cross section that were used to obtain the absolute differential cross sections. For the nuclides Nb, Mo, and Cd the coefficients B_1 and B_2 show a very smooth variation with energy, while B_3 is very close to zero throughout most of the energy range. The results indicate, therefore, that the scattering proceeds mainly through the interaction of S - and P -wave neutrons with

the nuclei involved with D -wave neutrons making a non-negligible contribution only near the upper limit of the energy range. These conclusions are consistent with the observed behavior of the coefficients C_1 , C_2 , and C_3 . The coefficients B_4 (which are obtained as a rigid fit to five Legendre polynomials) and C_4 are very small except near the upper limit of the energy range of interest. The fact that the polarization measurements (Fig. 1) show reasonably smooth energy and angular dependence is reflected in the lack of fluctuations in the energy dependence of the coefficients C_L .

The coefficients B_L and C_L for Zr show more rapid variations with energy. This is in agreement with the results in Fig. 1. Even for the case of Zr, the interaction of neutrons with orbital angular momentum $l \geq 2$ appears to be small. It is expected that averaging the products $P_2(\theta)\sigma(\theta)$ over larger energy intervals would lead to values of C_L that would vary more smoothly with energy.

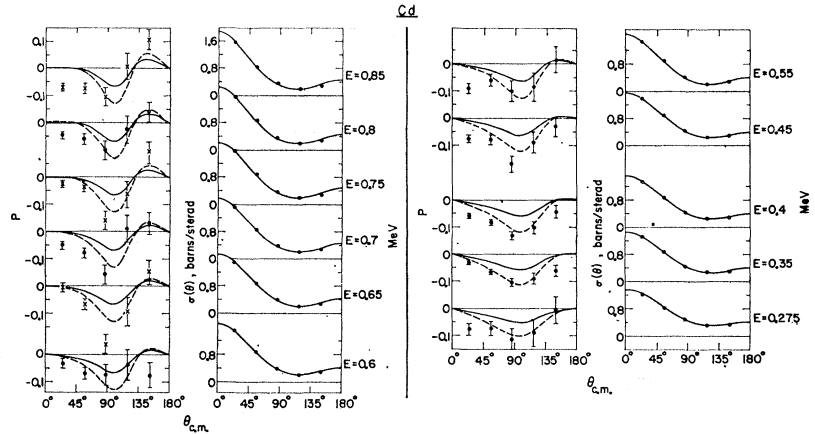
B. Optical-Model Analysis

1. General Discussion

The present measurements of both the polarization and the differential cross section vary reasonably smoothly with both energy and angle. This suggests that a description of the data in terms of an optical model might lead to a consistent interpretation of all the results, at least on the average.

A recent approach to a more nearly complete optical-model description of the scattering of nucleons from nuclei is the nonlocal model proposed by Perey and Buck.¹⁴ This model has been found to account success-

FIG. 5. Polarization and differential cross section for neutrons scattered from Cd, plotted as a function of angle at each incident-neutron energy. The solid circles and the \times 's are the experimental results, corrected for multiple scattering as discussed in the text. The solid curves are the predictions (including compound elastic scattering) of the equivalent local model with the parameters as given in Table I. In particular, the parameters of the spin-orbit potential are $V_s=7.2$ MeV, $W_s=0$. The dashed curves, shown only where they differ from the solid curves, have been calculated for the values $V_s=14$ MeV, $W_s=0$.



fully for a wide variety of experimental data on neutron scattering. The energy dependence of the effective central potential is contained explicitly in this nonlocal model. In many cases, scattering data were fitted as well by a set of energy-independent nonlocal parameters (obtained entirely from fits to the differential cross sections of neutrons scattered from Pb at 7 and 14.5 MeV) as they were by a local model for which the parameters were allowed to vary in order to obtain the fit at each energy for which measurements were made.

In order to test the nonlocal model at energies below 1 MeV, we have compared the predictions of the model with the present results. Our calculations were carried out with a local potential whose parameters are equivalent to the nonlocal parameters given by Perey and Buck (Ref. 14, Table IV, p. 363) and determined from a numerical solution of the approximate relation given as Eq. (35) in Ref. 14. That this equation leads to a very close correspondence between the nonlocal potential and the equivalent local one has been stressed by Perey and Buck¹⁴ and discussed by Monahan and Elwyn.²⁸ A further discussion of the correspondence between the two potentials and calculations of both the polarization and differential cross sections arising from these potentials is found in the Appendix. It should be pointed out that Perey and Buck treat the nonlocality of the central potential only.

The equivalent local potential that was utilized has the form

$$U_L(r) = -V_L f_s(r) - iW_L f_D(r) + (V_s + iW_s)(\hbar/\mu\pi c)^2 \sigma \cdot \mathbf{1}(1/r)(d/dr)f_s(r), \quad (4)$$

where

$$f_s(r) = \{1 + \exp[(r-R)/a_s]\}^{-1}$$

and

$$f_D(r) = 4 \exp\left(\frac{r-R}{a_D}\right) / \left[1 + \exp\left(\frac{r-R}{a_D}\right)\right]^2.$$

Here a_s is the diffuseness of the nuclear surface for the real well, a_D plays the same role for the imaginary central potential, $R=r_0 A^{1/3}$ is the nuclear radius, V_L and W_L are the real and imaginary depths of the equivalent local well, and V_s and W_s are the real and imaginary depths of the spin-orbit potential. In this form for the optical potential, the absorption is peaked on the nuclear surface, as is the spin-orbit potential which is of the Thomas derivative type.

The various equivalent local parameters for each of the incident energies utilized in the present experiment are listed in Table I, and the nonlocal parameters of Perey and Buck are given in the caption. Although the table gives the parameter values that were actually used, the energy dependence of the central potential is such that within the interval of energy and mass considered here the calculation can be successfully reproduced with the following central potential strength parameters, $V_L=47$ MeV and $W_L=9.6-9.8$ MeV.

TABLE I. Equivalent local parameters as a function of incident-neutron energy for Zr, Nb, Mo, and Cd. The notation is the same as in Eq. (4) in the text. The nonlocal parameters of Perey and Buck (Table IV of Ref. 14) are $V_N=71$ MeV, $W_N=15$ MeV, $r_0=1.22$ F, $a_s=0.65$ F, $a_D=0.47$ F, and $V_s=7.2$ MeV. [This value of V_s in the notation of Eq. (4) is equivalent to the value $U_{so}=1300$ MeV given by Perey and Buck.] The remaining parameters were constant at all energies for all four nuclei. The values are: $r_0=1.27$ F, $a_s=0.66$ F, $a_D=0.47$ F, $V_s=7.2$ MeV, and $W_s=0$.

Energy (MeV)	V_L (MeV)				W_L (MeV)			
	Zr	Nb	Mo	Cd	Zr	Nb	Mo	Cd
0.275	47.11	47.11		47.09	9.63	9.63		9.77
0.35	47.09	47.09		47.06	9.63	9.63		9.76
0.4	47.07	47.07	47.07	47.05	9.62	9.62	9.63	9.76
0.45	47.06	47.06	47.06	47.04	9.62	9.62	9.62	9.76
0.51	47.04	47.04	47.04	47.04	9.62	9.62	9.62	
0.55	47.03	47.03	47.03	47.01	9.61	9.61	9.62	9.75
0.6	47.02	47.02	47.01	46.99	9.61	9.61	9.62	9.75
0.65	47.00	47.00		46.98	9.61	9.61		9.75
0.7	46.99	46.99	46.98	46.96	9.61	9.61	9.61	9.74
0.75	46.97	46.97		46.95	9.60	9.60		9.74
0.8	46.96	46.96	46.95	46.93	9.60	9.60	9.60	9.74
0.85	46.95	46.94	46.94	46.92	9.60	9.60	9.60	9.73

²⁸ J. E. Monahan and A. J. Elwyn, Argonne National Laboratory Report ANL-6666, 1962 (unpublished).

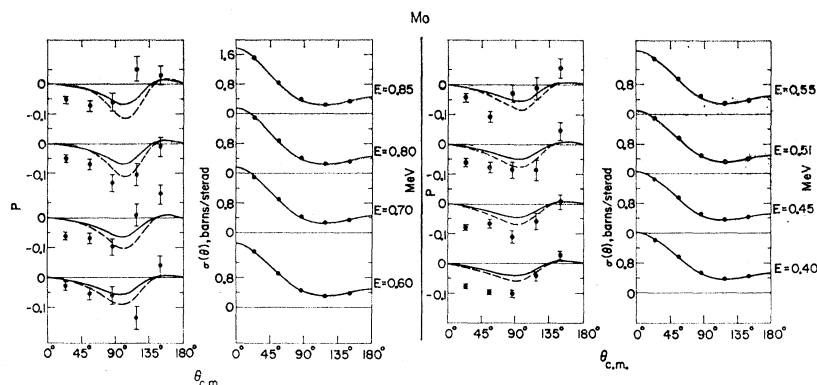


FIG. 6. Polarization and differential cross sections for neutrons scattered from Mo, plotted as a function of angle at each incident-neutron energy. Comments concerning the experimental points and the calculated curves are the same as for Fig. 5.

The calculations of polarization and differential cross section were performed on an IBM-704 computer by use of the code ABACUS-2.²⁹ All of the calculations have been corrected for the effects of compound elastic scattering by use of the formalism of Hauser and Feshbach³⁰; these corrections were also performed by the ABACUS-2 code. Inelastic scattering has been assumed to be completely negligible in all these calculations.

2. Comparison with the Nonlocal Model

The calculations are compared with measurements in Figs. 5 through 8. The experimental points on these figures have been corrected for multiple scattering as described above. The solid curves are the results of calculations (including compound elastic effects) based on the parameter values given in Table I; the dashed curves, shown only where they differ from the solid curves, correspond to the same parameter values except that the real spin-orbit well depth has been increased to $V_s = 14$ MeV.

The agreement between calculated and measured differential cross sections is excellent for the cases of Cd and Mo (Figs. 5 and 6). The polarization calculations are also in good agreement with the measurements, especially with the larger spin-orbit potential (14 MeV), except perhaps at the smaller angles in a number of cases. This discrepancy at small angles exists at many energies for all of the nuclei studied in the present work. Even with the larger spin-orbit potential, the present model does not account for the polarization measurements at 24° in a systematic manner. This point will be discussed further in Sec. IV.B.3; here it suffices to note that a supplementary experiment to investigate possible systematic errors in these small-angle measurements at one energy (0.7 MeV) indicated that the original results were indeed correct within statistical accuracy. Thus, the discrepancy is believed to be real.³¹

For the case of Nb (Fig. 7) the calculated values of the differential cross sections lie slightly above the measured values for most cases, although the general shapes of the calculated curves are consistent with the measured distributions. The polarization measurements, on the other hand, have much larger absolute values than those calculated, and in some cases differ in sign. Furthermore, increasing the real spin-orbit potential (from 7.2 to 14 MeV) has very little effect on the calculated polarizations.

As pointed out in Sec. IV.A above, both the sign and the magnitude of the measured polarizations of neutrons scattered from Zr change rapidly as a function of incident energy. We further suggested that this behavior might be explained in terms of the lower level density in nuclei near a magic number. In this case the optical-model calculations are not expected to agree with the observed results. Figure 8 shows the comparison. Although the measured and calculated values of the polarization agree only poorly, the differential cross sections agree in general shape. As with Nb, however, the measured cross sections at all energies (except 0.275 MeV) appear to lie slightly above the calculated curves.

In the hope of smoothing out the observed fluctuations in the polarization, the Zr measurements were

clear Coulomb field—according to the plane-wave Born approximation theory developed by Schwinger [Phys. Rev. **73**, 407 (1948)]. The resulting polarizations vary from -0.035 to -0.045 for neutrons scattered from Zr, Nb, Mo, and Cd at a scattering angle of 24° . When the experimental results are “corrected” for this effect the polarizations at 24° due only to the nuclear spin-orbit force are in somewhat better agreement with the predictions of the equivalent local model. The plane-wave Born approximation however is thought to yield absolute values that are too large at angles as large as 20° . Baz [Zh. Eksperim. i Teor. Fiz. **31**, 159 (1956) [translation: Soviet Physics—JETP **4**, 259 (1957)]] using an approach which is believed to be somewhat more realistic for large angles finds somewhat lower absolute values of the polarization. Because we feel that the Schwinger approximation gives an upper limit only to the size of the effect, the measured values of the polarization at 24° shown in the figures have not been modified. In Fig. 10, however, we do include the modified as well as the original values as an indication of the size of the effect. Further work toward a more realistic calculation for angles greater than 20° is in progress. We would like to thank Professor S. E. Darden for suggesting to us that the effect of the electromagnetic spin-orbit interaction might be somewhat larger than we had at first anticipated.

²⁹ E. H. Auerbach, Brookhaven National Laboratory Report BNL-6562, 1962 (unpublished).

³⁰ W. Hauser and H. Feshbach, Phys. Rev. **87**, 366 (1952).

³¹ We have calculated the polarization that is expected due to the electromagnetic spin-orbit interaction—the spin-orbit interaction arising from the motion of the neutron magnetic moment in the nu-

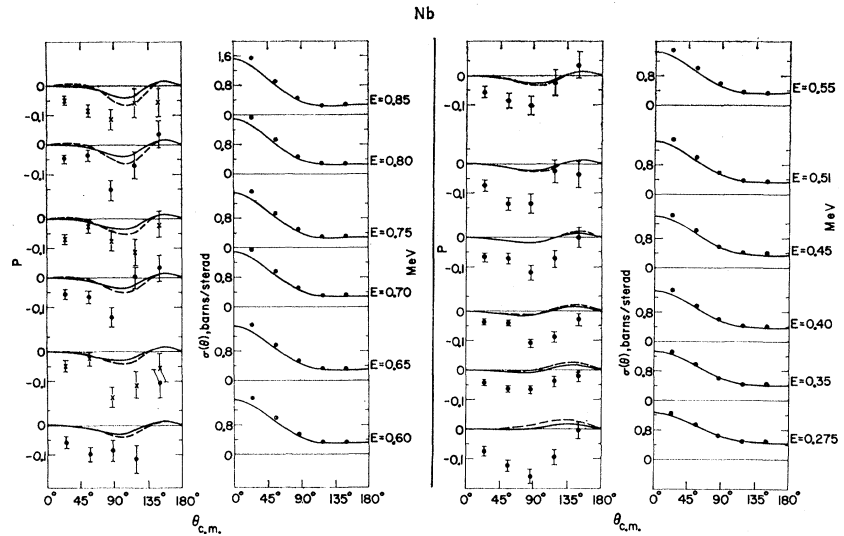


FIG. 7. Polarization and differential cross section for neutrons scattered from Nb, plotted as a function of angle at each incident-neutron energy. Comments concerning the experimental points and the calculated curves are the same as for Fig. 5.

averaged numerically over a larger energy interval. The intervals were chosen as 0.35–0.45 MeV, 0.45–0.55 MeV, 0.55–0.65 MeV, 0.65–0.75 MeV, and 0.75–0.85 MeV. Figure 9 shows the resulting values for both polarization and differential cross sections. As can be seen, many of the previous fluctuations have disappeared and the polarization varies reasonably smoothly with energy. In this figure, the solid curves were calculated with the parameters in Table I except that the value of the real spin-orbit potential was increased to $V_s = 10$ MeV. (This gives results negligibly different from those with $V_s = 7.2$ MeV.) The dashed curves were calculated with the same parameters as the solid curves except that the imaginary central potential W_L has been arbitrarily reduced in magnitude by 25% from the values in Table I. Such a reduction in W_L might be justified³² for nuclei near the

magic numbers because of the reduced level densities. This reduction improves the agreement between the calculated and the measured values of the differential cross sections. The calculated values of the polarization are increased at the larger angles, but the agreement with the averaged measurements is not appreciably improved.

Calculations with the value of W_L reduced by 25% from the values given in Table I have also been made for Nb. As with Zr, the agreement with the measured differential cross sections is improved but the general agreement with the polarization measurements is substantially unaffected. The justification of a reduction of the imaginary central potential well depth for a nuclide such as Nb in terms of its nuclear shell structure is not as obvious as for Zr.

The total neutron cross sections calculated from the

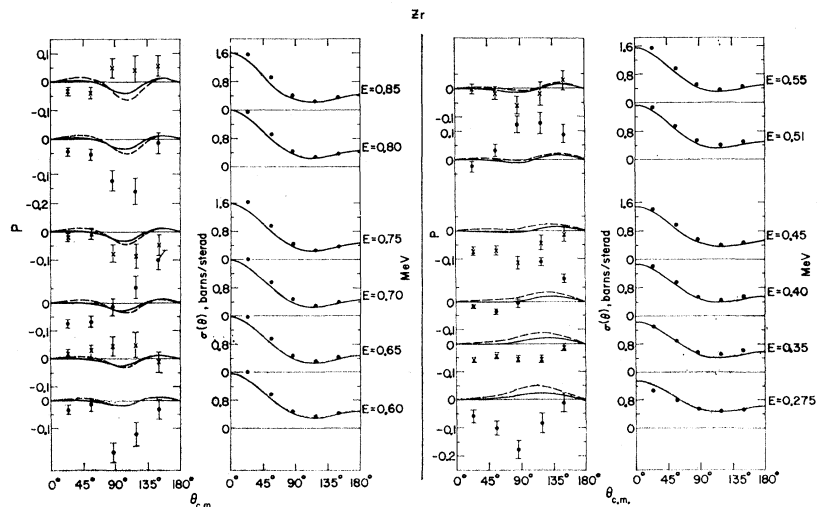


FIG. 8. Polarization and differential cross section for neutrons scattered from Zr, plotted as a function of angle at each incident-neutron energy. Comments concerning the experimental points and calculated curves are the same as for Fig. 5.

³² A. M. Lane, J. E. Lynn, E. Melkonian, and E. R. Rae, Phys. Rev. Letters 2, 424 (1959).

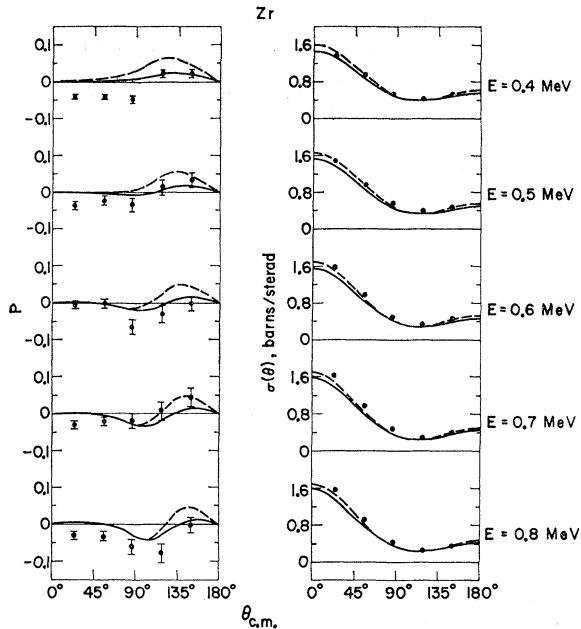


FIG. 9. Angular dependence of the polarization and differential cross sections for neutrons scattered from Zr. These results differ from those in Fig. 8 in that the data were averaged over a larger energy interval. The solid curves are the predictions of the equivalent local model with the parameters in Table I, except that the strength of the spin-orbit potential well is $V_s=10$ MeV. The dashed curves are the same as in Fig. 8 except that the value of the imaginary central-potential well strength W_L was made 25% smaller than the values given in Table I.

equivalent local model (with the parameters in Table I) are in excellent agreement with the measured values shown in the compilation BNL-325²⁰ for both Mo and Cd. (There is very little change when V_s is increased to 14 MeV.) For both Zr and Nb, the calculated values of σ_T are about 15% below a smooth curve drawn through the measured values in BNL-325. Reducing the imaginary well depth W_L of the central potential by 25%, as discussed above, leads to much better agreement between calculations and the average of the compilation values of σ_T for Zr and Nb.

In summary, the data have been analyzed in terms of a local model equivalent to the nonlocal model of Perey and Buck. When compound-nucleus effects are taken into account in a consistent fashion, the calculations are in good general agreement with the measurements, especially for the differential cross section. For these latter measurements, the model gives an excellent description of the results for Cd and Mo. For Zr (the averaged results) it appears that the differences between the measurements and calculations can be understood qualitatively in terms of nuclear shell-structure effects. For Nb, the model gives a consistent explanation of the shape of the observed differential cross section, although a slightly lower value of W_L improves the agreement in magnitude.

Except at the smallest angles, the calculated polariza-

tions for Cd are in reasonable agreement with the measurements, and again, except at the smallest angles, there is at least qualitative agreement for Zr (averaged data) and for Mo. For Nb, the calculated polarizations at all angles appear to be systematically smaller (in absolute value) than the measured ones. Although it does appear to be an adequate description for some of the data, the model does not account consistently for the polarization measurements at angles less than 90° in all four nuclei. This remains true even when the modifications due to the electromagnetic spin-orbit force³¹ have been considered.

3. Inclusion of an Imaginary Spin-Orbit Potential

The value of the polarization should be particularly sensitive to the magnitude and form of the spin-orbit potential. In an effort to better understand the polarization measurements, we have made preliminary attempts to modify both the real and imaginary spin-orbit terms in the potential shown in Eq. (4). Because the equivalent local model gave a generally excellent description of the differential cross section, we retained the central-potential parameters shown in Table I.

With a real well depth $V_L=47$ MeV for the central potential, the real spin-orbit potentials $V_s=7.2$ and 14 MeV used in the previous analysis correspond to Thomas factors³³ $\lambda=27.7$ and 53.8, respectively. Ross *et al.*³⁴ have shown that good level sequence and shell structure for bound single-particle states of nucleons moving in a diffuse potential of the Woods-Saxon type is consistent with a value of $\lambda=39.5$ (for a real central-potential well depth $V_L=43$ MeV). For $V_L=47$ MeV, this value of λ would correspond in our notation to $V_s=10.3$ MeV. The value $V_s=10$ MeV employed in the following analysis is completely consistent with the value of λ obtained by Ross *et al.*

The results discussed in the preceding pages were obtained for an imaginary spin-orbit potential W_s equal to zero. There is no *a priori* reason why the spin-orbit force should not be complex.³⁵ Analyses of previous work at

³³ The parameter λ is a measure of the strength of the real spin-orbit potential in the Thomas form for the radial dependence. That is, the spin-orbit force term in the optical potential can be written

$$\lambda V_L \left[\frac{\hbar^2}{4m^2c^2} \right] \frac{1}{r} \frac{d}{dr} f_s(r) \sigma \cdot \mathbf{l},$$

where V_L is the real well depth of the central potential.

³⁴ A. A. Ross, H. Mark, and R. D. Lawson, Phys. Rev. **102**, 1613 (1956).

³⁵ The significance of an imaginary spin-orbit potential is discussed in Ref. 15. In particular, the condition given in Eq. (9) of this reference must be satisfied for all values of j , where $j=l \pm \frac{1}{2}$, in order that the total potential not act as a source of neutrons in any "channel" j . In the present calculations this condition is satisfied over an interval $R-2a_s \leq r < \infty$ for $l < 7$. We find that outside of this radial interval the imaginary part of the potential, in our Eq. (4), can be set equal to zero without materially affecting the calculated results. Furthermore, the contribution from partial waves corresponding to values of l greater than 2 are entirely negligible. Therefore, as far as the present calculations are concerned, the introduction of an imaginary spin-orbit term in the phenomenological optical-model potential simply implies that for any given value of l the probability for neutron absorption depends on j .

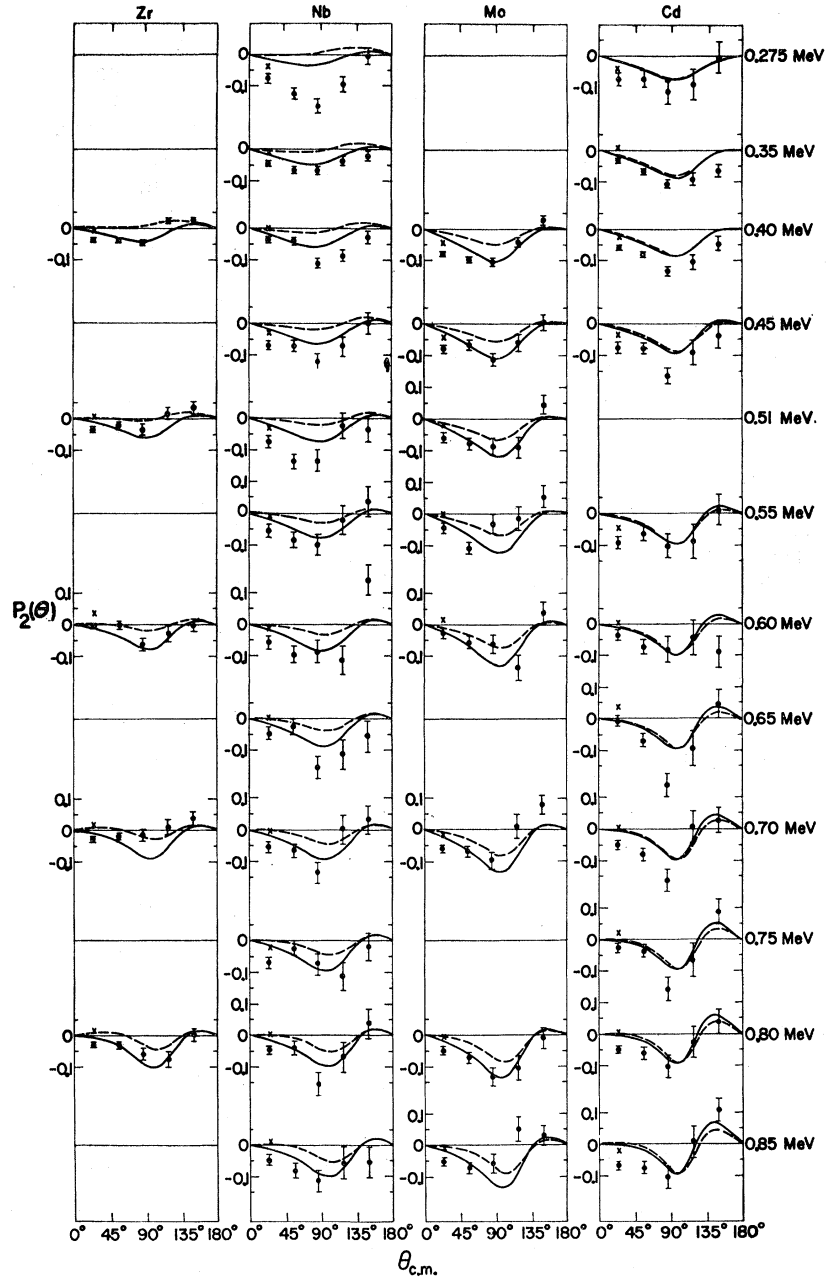


FIG. 10. The angular dependence of the polarization $P_2(\theta)$ for each incident-neutron energy for the four nuclides Zr, Nb, Mo, and Cd. The solid curves are the predictions of the equivalent local model except that both a real and an imaginary spin-orbit potential are employed with $V_s=10$ MeV and $W_s=4$ MeV. The dashed curve differs only in setting $W_s=0$. The data points for Zr are average values (see Fig. 9). The \times 's are the values of the polarization due to nuclear forces only, when the effects of the electromagnetic spin-orbit interaction, as explained in Ref. 31, have been approximately accounted for.

low energies usually have omitted the imaginary term simply on the grounds that it was not necessary in order to achieve adequate agreement with the data.⁴ We have found however that the use of an imaginary as well as a real term to describe the spin-orbit potential leads to a considerably more consistent interpretation of the polarization, at least within the framework of the Perey-Buck model, for nuclei near $A=100$, even for energies below 1 MeV.

Figure 10 compares the measured polarization with

that calculated both with and without an imaginary term in the spin-orbit potential. The solid curves were calculated with the parameters given in Table I except that $V_s=10$ MeV and $W_s=4$ MeV. The dashed curves differ from the solid ones only in setting $W_s=0$. The differences between the differential cross sections calculated with these two sets of parameters are completely negligible, and both agree with the data as well as did the calculations shown in Figs. 5 through 8.

As shown, the agreement between the measured and

calculated values for Nb is substantially improved by the inclusion of the imaginary spin-orbit term. In fact, except at 0.275 MeV and a few other points, the agreement is quite close. Even the measurements at the smallest angle (24°) (with or without the inclusion of the effect of the electromagnetic interaction) are for the most part in better agreement with the calculations that include the imaginary spin-orbit term. For Mo, the calculations involving the imaginary spin-orbit term are at least as consistent with the data as the calculations without it, and certainly the polarizations at angles less than 90° calculated with an imaginary spin-orbit term agree more closely with the measurements than do those employing only a real potential. For Cd, the two sets of calculations are practically indistinguishable, either set being in reasonable agreement with most of the data. For Zr, employing both a real and an imaginary potential does not make the calculations less consistent with the averaged data.

No attempt has been made to determine a "best set" of values for the parameters. It is not clear at present whether the deviations of the data from the calculations are due to effects of fluctuations in the compound nuclei that cannot be explained in terms of an averaged-potential model, or whether these data could be fitted somewhat more satisfactorily by further variation and/or modification of the parameters that characterize such a potential. Since polarization is an interference phenomenon, the effects of fluctuations in the compound nucleus are probably reflected more sensitively in neutron polarizations than in angular distributions, and possibly polarization measurements should not be expected to agree as well with any optical-model calculations as the measurement of the unpolarized differential cross sections do. It does appear clear, however, that any consistent set of calculations describing the present data and *utilizing a local optical model equivalent to the model of Perey and Buck* should involve both a real and an imaginary spin-orbit potential—at least if such a potential is of the Thomas form.

There is presumably no direct theoretical requirement that the nuclear spin-orbit potential have the Thomas form.¹³ Further investigation of the shape of this potential would be of interest. We have made a preliminary attempt to fit the data in a consistent manner by use of a real volume spin-orbit potential. This form had the same radial dependence as the real central potential. Under these conditions and with values of the central-potential parameters given by the equivalent local model, a value $V_s \approx 2$ MeV produced results in agreement with the neutron total cross sections. However, the agreement with the polarization measurements for Zr and Nb was significantly poorer for these calculations than for the corresponding calculations previously discussed. The calculations for Mo and Cd were much less consistent over the whole energy range studied than were the previous calculations, especially at the forward angles. On the other hand, the comparison between these calculations

and the measured differential cross sections showed qualitative agreement for all of the nuclides over the entire energy range of the present experiment. This last point emphasizes again that a meaningful choice among optical-model descriptions can be made only by the simultaneous fitting of total cross sections, angular distributions, polarizations, and possibly other measurements—not just by the consideration of any one set of data alone.

4. Neutron Strength Functions

Most optical-model descriptions of neutron scattering predict a maximum in the P -wave strength function in the neighborhood of mass $A = 100$. Experimental measurements,^{36,37} although of poor statistical accuracy, verify the existence of this resonance and indicate that the peak is somewhat asymmetric. It has been suggested³⁶ that the measurements actually show fine structure and that this splitting can be interpreted as due to the spin-orbit force which divides the $3P$ resonance into a $P_{3/2}$, $P_{1/2}$ doublet. Several attempts^{38,39} have been made to estimate the strength of the spin-orbit potential from an analysis of the data on this P -wave strength function.

We have calculated the P -wave strength function⁴⁰ by use of the parameters predicted by the equivalent local model for nuclides with mass numbers between 70 and 130. Figure 11 compares these calculations with the data. The dashed curve was calculated with the values $V_s = 7.2$ MeV and $W_s = 0$ (the same values as in Figs. 5 through 8). This curve supports the conclusion of Buck and Perey⁴¹ who find that the normal spin-orbit potential has a negligible effect on the width and magnitude of the resonance; that is, it certainly does not split the

³⁶ L. W. Weston, K. K. Seth, E. G. Bilpuch, and H. W. Newson, *Ann. Phys. (N.Y.)* **10**, 477 (1960).

³⁷ A. K. Furr, H. W. Newson, and B. H. Rohrer, *Ann. Phys. (N.Y.)* (to be published); A. Saplakoglu, L. M. Bollinger, and R. E. Coté, *Phys. Rev.* **109**, 1258 (1958); F. Boreli and S. E. Darden, *ibid.* **109**, 2079 (1958); J. S. Desjardins, J. L. Rosen, W. Wiltrens, and J. Rainwater, *ibid.* **120**, 2214 (1960); J. L. Rosen, S. Desjardins, W. W. Havens, and J. Rainwater, *Bull. Am. Phys. Soc.* **4**, 473 (1959).

³⁸ H. Fiedeldey and W. E. Frahn, *Ann. Phys. (N.Y.)* **19**, 428 (1962).

³⁹ T. K. Krueger and B. Margolis, *Nucl. Phys.* **28**, 578 (1961).

⁴⁰ We define the neutron strength function for relative angular momentum l in terms of the optical-model transmission coefficients T_l^j by the relation

$$\bar{S}_l = \frac{1}{4\pi P_l} \left[\frac{(l+1)T_l^{l+1/2} + lT_l^{l-1/2}}{2l+1} \right],$$

where P_l is the barrier penetrability for angular momentum l . The quantity \bar{S}_l^p which is plotted (for $l=1$) in Fig. 11 is related to \bar{S}_l by the relation

$$\bar{S}_l^p = \frac{2kR}{E_0^3} \bar{S}_l,$$

where k is the wave number at energy E_0 , R is the nuclear radius, and E_0 is the neutron center-of-mass energy in eV. (See Saplakoglu *et al.*, Ref. 37.)

⁴¹ B. Buck and F. Perey, *Phys. Rev. Letters* **8**, 444 (1962).

resonance into two peaks nor does it affect the asymmetry significantly. The solid curve in Fig. 11 was calculated with $V_s=10$ MeV and $W_s=4$ MeV (the same values as in Fig. 10). The difference between the two curves is seen to be very small. It can be shown furthermore that the calculated strength function is changed only slightly by increasing the strength of the spin-orbit coupling by an additional factor of two or three as long as we retain the above values for the parameters that describe the central potential. For example, the dotted curve in Fig. 11 represents a calculation based on the values $V_s=20$ MeV and $W_s=0$. The peak has shifted to slightly lower values of A , and is perhaps more asymmetric than the solid or dashed curves. However, there is no indication of a splitting into two peaks in this region of A . Including an imaginary spin-orbit term of strength $W_s=7.2$ MeV in the last calculation tends to flatten the resulting resonance, but otherwise the shape of the peak is not significantly altered.

Thus, for central potentials with the strengths predicted by the local model equivalent to the Perey and Buck nonlocal model, both the magnitude and shape of the $3P$ strength-function resonance are practically independent of the value of the spin-orbit potential. Therefore, if this model is a realistic one the possible splitting of the $3P$ resonance cannot be attributed to a spin-orbit interaction. The fact that the present model leads to a reasonably consistent interpretation of the scattering measurements would seem to indicate that the strengths $V_L=47$ MeV, $W_L\approx 10$ MeV used for the central potential may be more realistic than nonunique values obtained by the use of a fitting procedure at each neutron energy. If such is the case, then some other mechanism, such as the effect of collective motions,⁴¹ must be responsible for any splitting of the $3P$ resonance.

In any event, the shape of the giant resonance depends sensitively on the strength of the spin-orbit potential *only for certain values of the imaginary potential* W_L . This fact has not been sufficiently stressed in previous work. For V_L still in the neighborhood of 47 MeV but with W_L reduced to 3 MeV, doubling the spin-orbit strength from $V_s=10$ MeV to 20 MeV splits the calculated $3P$ resonance into two distinct peaks. This is in agreement with the conclusions of Krueger and Margolis³⁹ who use an imaginary central potential which reaches its maximum value of about 1.5 MeV near the nuclear surface. Obviously, these results depend critically on the imaginary part of the central potential and can lead to unambiguous predictions only if the value of W_L is somehow fixed in an independent manner.

Finally, it should perhaps be mentioned that in the mass-number region $70\leq A\leq 130$ the S -wave neutron strength functions calculated from the present model are somewhat larger than the measured ones. Moldauer,¹³ employing his local optical model with a diffuse surface and a sharply peaked absorptive shell at the surface, obtains a better fit to the S -wave data. The model of Moldauer, incidentally, utilizes imaginary central-poten-

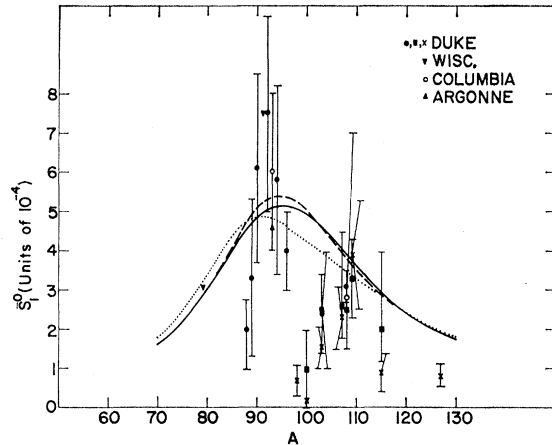


FIG. 11. The P -wave neutron strength functions (Ref. 40) plotted against mass number in the region $70\leq A\leq 130$. The data points were taken from Refs. 36 and 37. The solid curve represents the prediction of the equivalent local model with the parameters as given in Table I except $V_s=10$ MeV and $W_s=4$ MeV. The dashed curve is the same except $V_s=7.2$ MeV and $W_s=0$; the dotted curve differs from the dashed one only in that $V_s=20$ MeV. The results shown here were calculated for a neutron energy of 0.2 MeV. Similar calculations for 0.05 MeV were 10–20% larger in magnitude in the mass number region $88\leq A\leq 120$, but yielded the same over-all resonance shapes.

tial well depths of 10–14 MeV and a real well depth of 46 MeV. These parameters are, therefore, not too different from the equivalent local parameters of the present model. His results also confirm the conclusion that for values of W_L near 10 MeV the P -wave strength function is not very sensitive to the values of V_s , the real well depth of the spin-orbit potential. The polarizations calculated with the Moldauer model are in qualitative agreement with the measurements described in the present paper.

Some modification of the present model could be usefully studied. In particular, the radial dependence of the imaginary central potential should be investigated in order to study the effects of the fringe absorption suggested by Moldauer.^{13,42} With the present model as a starting point, further adjustments of the radial dependence of the real and imaginary spin-orbit potential might be fruitful. It is felt that reasonable modifications of the model would not seriously affect the generally consistent interpretation of the scattering data, both angular distributions and polarizations.

ACKNOWLEDGMENTS

The authors wish to express their appreciation to Dr. F. Perey and Dr. B. Buck for providing them with calculations based on their nonlocal optical model. We further acknowledge the many useful discussions with Dr. Peter Moldauer. We also wish to thank S. Zawadski for his assistance in using the optical-model code ABACUS-2, D. Mueller for his help with reducing the data, and

⁴² P. Moldauer, Phys. Rev. Letters **9**, 17 (1962).

W. Ray, R. Amrein, and the Van de Graaff crew for their assistance in performing the experiment.

APPENDIX

Perey and Buck¹⁴ have shown that a local potential $U_L(r)$ approximately equivalent⁴³ to their nonlocal potential $U_N(r)$ is related to the latter by the expression

$$U_L(r) \exp\{M\beta^2[E - U_L(r)]/(2\hbar^2)\} = U_N(r). \quad (\text{A1})$$

The length β is a measure of the range of nonlocality and

$$-U_N(r) = V_N f_s(r) + iW_N f_D(r). \quad (\text{A2})$$

The notation is identical to that in Ref. 14. In particular, $f_s(r)$ is the Saxon-Woods form factor and $f_D(r)$ is a surface absorption term of the Saxon derivative type. All of the parameters in Eq. (A2), including the radius and diffuseness parameters in $f_s(r)$ and $f_D(r)$, have been evaluated by Perey and Buck. We therefore consider the function $U_N(r)$ to be completely specified.

Instead of evaluating $U_L(r)$ for a sequence of values of r directly by use of the transcendental equation (A1),

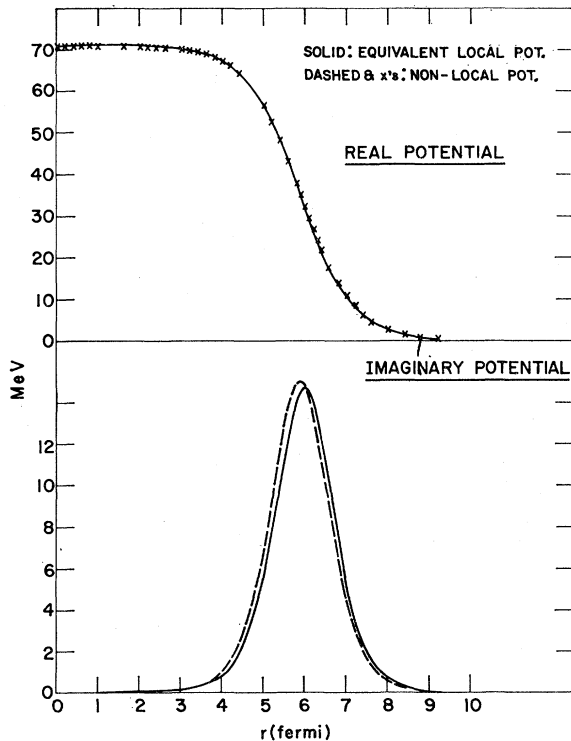


FIG. 12. A comparison of the equivalent local potential (solid curves) and the nonlocal potential of Perey and Buck (x's and dashed curves). The equivalent local potential was determined by using the approximation (A3) in Eq. (A1) as explained in the Appendix.

⁴³ For a given value of total energy E , an equivalent local potential can be defined as a potential for which the logarithmic derivative of the solution of the local wave equation is asymptotically equal to the logarithmic derivative of the solution of the corresponding nonlocal equation.

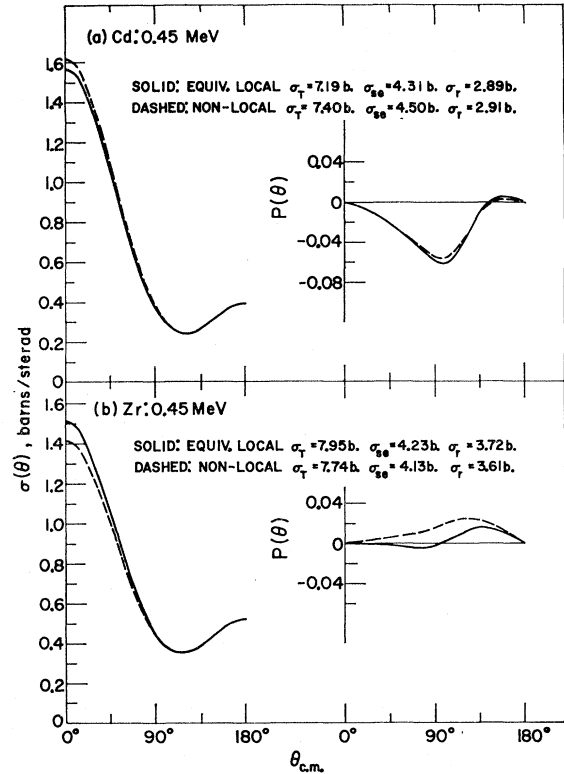


FIG. 13. A comparison of the polarization and differential cross section calculated from the equivalent local potential and from the nonlocal potential of Perey and Buck. These calculations have been corrected for compound elastic scattering. Curve (a) was calculated for neutrons scattered from Cd at 0.45 MeV; curve (b) is for neutrons scattered from Zr at 0.45 MeV. Also shown in the two cases are the predicted values of the total cross section σ_t , shape elastic-scattering cross section σ_{se} , and reaction cross section σ_r .

we found it more convenient to proceed as follows. We assume for $U_L(r)$ a functional form that contains a number of adjustable parameters. The values of these parameters are then determined such that the resulting function $U_L(r)$ is an approximate solution to Eq. (A1) for all values of the radial coordinate r . In particular, $U_L(r)$ was assumed to be of the form

$$-U_L(r) = V_L / \left[1 + \exp\left(\frac{r-x}{y}\right) \right] + 4iW_L \exp\left(\frac{r-x}{a_D}\right) / \left[1 + \exp\left(\frac{r-x}{a_D}\right) \right]^2, \quad (\text{A3})$$

where the values of V_L , W_L , x and y are to be determined such that Eq. (A1) is satisfied as nearly as possible (in the sense of least squares) over the entire interval of r for which $U_L(r)$ is significantly different from zero.⁴⁴ Equation (A3) has the same functional form as Eq.

⁴⁴ A Fortran II code for this calculation has been written for the IBM-704 computer. A description of this code will be supplied on request.

(A2) and the value of a_D in Eq. (A3) is assumed to be equal to the value of the corresponding parameter in the nonlocal potential. The resulting local potential $U_L(r)$, modified by the addition of a spin-orbit term, is used as described in Sec. IV.B.1 to calculate the various optical-model cross sections. The approximation (A3) is particularly convenient since it can be used without modification in existing optical-model computer programs. In Fig. 12, the equivalent local potential determined by substituting approximation (A3) in Eq. (A1) is compared with the nonlocal potential given by Eq. (A2).

For those cases for which all requisite calculations were made, the values of the differential cross section and polarization calculated by use of the approximation (A3) agreed slightly better with the predictions of the actual nonlocal model of Ref. 14 than did values calcu-

lated directly by use of Eq. (A1). In fact the differences between calculations based on Eq. (A3) and those based on the nonlocal model of Perey and Buck were small enough that they might reasonably be ascribed to differences in numerical routines in the two computer codes. The differential cross sections and polarizations calculated by these methods are compared in Fig. 13.

As far as agreement with the observed data is concerned, it seems reasonable to think of Eqs. (A1) and (A3) as constituting a "model" quite independent of their relation to the original nonlocal model. However, the results described in the previous paragraph indicate that such a distinction is not necessary and, in particular, that Eq. (A3) is an adequate approximation to an equivalent local potential for the ranges of energy and mass number of concern here.

Average Energy and Angular Momentum Removed from Dy Compound Nuclei by Neutrons and Photons*

JOHN M. ALEXANDER† AND GABRIEL N. SIMONOFF‡

Lawrence Radiation Laboratory, University of California, Berkeley, California

(Received 7 June 1963)

Excitation functions are presented for many heavy-ion-induced (HI) reactions that produce Dy^{149} , Dy^{150} , and Dy^{151} . Projectiles were C^{12} , N^{14} , N^{15} , O^{16} , O^{18} , F^{19} , Ne^{20} , and Ne^{22} of 4 to 10.4 MeV per amu. The reactions studied are all of the type (HI, xn) , where x ranges from 3 to 11. A large fraction of the total reaction cross section is accounted for by these (HI, xn) reactions—0.9 at approximately 45 MeV to 0.4 at approximately 120 MeV. An analysis to obtain the energy of the first emitted neutron is presented. Comparison of the results of this analysis to angular-distribution studies suggests that the first neutron removes 2 to $4\hbar$ units of angular momentum. We obtain the relationship between average total photon energy and average angular momentum removed by photons. Comparison with the average individual photon energy from other work leads to an average of $1.8 \pm 0.6\hbar$ for the angular momentum removed by each photon. The excitation energy E_j of the lowest lying state of spin J has been estimated.

I. INTRODUCTION

CURRENTLY available beams of heavy ions (HI) make it possible to study compound nuclei over a wide range of excitation energy and angular momentum. Radiochemical studies are quite useful because they give information about specific reactions; e.g., the $(\text{HI}, 5n)$ reaction can be studied without interference from the reactions $(\text{HI}, 6n)$, $(\text{HI}, p5n)$, etc. This specificity is difficult to obtain by physical means because of complex coincidence-detection requirements. The products Tb^{149g} , Dy^{150} , and Dy^{151} have been extensively studied because they can be easily identified by their characteristic alpha radioactivity.

In previous studies we have presented recoil-range

data that give strong evidence that these products are produced by essentially pure compound-nucleus reactions.¹⁻³ Also reported are angular-distribution measurements from which it has been possible to obtain the average total energies (T_n and T_γ) of neutrons and photons.³

The experimental data reported here consist of excitation functions for 36 reactions of type $(\text{HI}, xn)\text{Dy}^{149}$, $(\text{HI}, xn)\text{Dy}^{150}$, $(\text{HI}, xn)\text{Dy}^{151}$. Compound nuclei of masses 154 to 160 have been formed by various projectiles and targets.

The conventional treatment of excitation-function data involves the use of the statistical model with little, if any, allowance for the effect of angular momentum. This type of treatment may possibly be

* Work done under the auspices of the U. S. Atomic Energy Commission.

† Present address: Department of Chemistry, State University of New York at Stony Brook, Stony Brook, New York.

‡ Present address: Nouvelle Faculté des Sciences de Bordeaux, Talence (Gironde) France.

¹ L. Winsberg and J. M. Alexander, Phys. Rev. **121**, 518, 529 (1961).

² J. M. Alexander and D. H. Sisson, Phys. Rev. **128**, 2288 (1962).

³ G. N. Simonoff and J. M. Alexander, following paper, Phys. Rev. **133**, B104 (1964).